Review Article

Nano Research
2024, 17(9): 7830–7839

ISSN 1998-0124 CN 11-5974/O4
https://doi.org/10.1007/s12274-024-6779-y

Covalent triazine frameworks materials for photo- and electro-catalysis

Aoji Liang[1,§], Wenbin Li[1,§], Anbai Li[1], Hui Peng[1], Guofu Ma[1] (✉), Lei Zhu[2] (✉), Ziqiang Lei[1], and Yuxi Xu[3] (✉)

[1] *Key Laboratory of Eco-functional Polymer Materials of the Ministry of Education, Key Laboratory of Polymer Materials of Gansu Province, College of Chemistry and Chemical Engineering, Northwest Normal University, Lanzhou 730070, China*
[2] *School of Chemistry and Materials Science, Hubei Key Laboratory of Quality Control of Characteristic Fruits and Vegetables, Hubei Engineering University, Xiaogan 432000, China*
[3] *School of Engineering, Westlake University, Hangzhou 310024, China*
[§] *Aoji Liang and Wenbin Li contributed equally to this work.*

Received: 28 April 2024 / **Revised:** 21 May 2024 / **Accepted:** 22 May 2024

ABSTRACT

Covalent triazine frameworks (CTFs) are a class of unique two-dimensional nitrogen-rich triazine framework with adjustable chemical and electronic structures, rich porosity, good stability and excellent semiconductivity, which enable great various applications in efficient gas/molecular adsorption and separation, energy storage and conversion, especially photo- and electro-catalysis. Different synthesis strategies strongly affect the morphology of CTFs and play an important role in their structure and properties. In this concept, we provide a comprehensive and systematic review of the synthesis methods such as ionothermal synthesis, phosphorus pentoxide catalytic method, polycondensation and ultra-strong acid catalyzed method, and applications of CTFs in photo- and electro-catalysis. Finally we offer some insights into the future development progress of CTFs materials for catalytic applications.

KEYWORDS

covalent triazine frameworks, synthetic strategy, photocatalysis, electrocatalysis

1 Introduction

The increasing scale of industrial development has led to the massive consumption of non-renewable energy sources, posing an enormous set of energy and environmental challenges. In order to reduce dependence on fossil energy sources, it is imperative to urgently develop clean, green and sustainable energy sources to achieve the goal of carbon neutrality, which has received significant attention. Relative to these non-fossil energy resources, renewable energy sources are relatively more widely distributed in terms of inexhaustible and recyclable. In addition, photocatalysis and electrocatalysis driven by solar energy and electric energy, in particular, have become a key area of research and interest due to the convenience and rapidity in the use of light and electrical energy sources [1–4]. Specifically, valuable photocatalysts and electrocatalysts usually have abundant reaction sites and tunable properties [5–7]. However, most of the reported photocatalysts [8, 9] cannot meet these requirements due to the low structural tunability and low utilization of the metal atoms [10, 11], which greatly limits their applications in the real life.

Covalent organic frameworks (COFs) are a class of structurally ordered metal-free π-stacked layered organic porous materials with strong covalent bonding networks, which have the advantages of large specific surface area, tunable electronic structure, and good chemical stability, and thus have turned the attention of the field of vision towards it. As a branch of COFs, covalent triazine frameworks (CTFs) are a class of organic polymer porous materials consisting of aromatic 1,3,5-triazine rings, mostly amorphous, and with a few ordered structures, which are unique in that they are composed of a series of C=N connected triazine units. It has excellent physical properties, chemical stability and good stability thermal due to its strong planar π-conjugated nature of the aromatic rings. In 2008, Pierre Kuhn Dr et al. produced for the first time a porous covalent triazine-based skeleton in high temperature molten zinc chloride conditions by ionothermal reaction, then, triazine-based materials have since gained much popularity and attention [12]. Thanks to the rich pore structure, large specific surface area and excellent semiconductivity properties of their nitrogen-rich special triazine frameworks, it has found great applications as sensors in gas adsorption/separation, efficient energy storage and conversion and photo- and electro-catalysis particularly [13, 14]. With the deepening and strengthening of research, the application of CTFs in photo-electrocatalysis has become more and more popular, mainly due to the following reasons: (1) Compared to inorganic materials, CTFs are organic porous materials that are structurally tunable and can be pre-designed based on the structure, which have highly influential in the field of photocatalysis [15–17]; (2) the ordered conjugated π structure of CTFs endows their chemically and thermally stable in most catalytic reactions and easily recyclable, making them more suitable to act as catalytic reactants for photo- and electro-catalysis; (3) the high tolerance of the covalent skeleton to rigorous and harsh reaction treatments [18], leads to a tighter structural linkage between the precursor

Address correspondence to Guofu Ma, magf@nwnu.edu.cn; Lei Zhu, Lei.zhu@hbeu.edu.cn; Yuxi Xu, xuyuxi@westlake.edu.cn

and the carbonaceous product; (4) the large specific surface area and large pore structure make it more favorable for exposing more active sites, thus enhancing the catalytic ability of the reaction; (5) the special structure of the triazine framework can coordinate with transition metal atoms, and various heteroatoms can be introduced to "fix" the transition metal complexes by anchoring them to N-containing functional groups (triazine groups), forming a richer matrix structure of metal complexes for CTFs, which can inhibit large-scale agglomeration of metals. At the same time, its structural diversity can provide high-affinity binding sites for various guest species, which will lead to a wide range of applications for different catalysts [19, 20]. Therefore, CTFs have been developed as supercapacitor capacitive electrode materials and their semiconducting properties make them suitable to act as photocatalysts for CO_2 capture [21]. It can be seen that the nitrogen-rich triazine framework has brought light to the dawn of the new photoelectrically superior catalysts, but there are many challenges to be solved, such as low crystallinity, severe acid carbonation, and insufficient exposure of the active sites [22].

The paper summarizes the prevalent synthesis methods of CTFs, systematically illustrates the advantages and challenges of each method and the impact on the photo- and electro-catalytic performance. Meanwhile, the latest advances in the application of CTFs in CO_2 capture and photocatalytic hydrogen production are summarized in detail, and relevant strategies to improve the photocatalytic performance of covalent triazine skeletons are briefly outlined. In addition, the application of CTFs-based materials in electrocatalysis has also been mentioned for research in recent years. We hope to provide some future expected design guidance directions for synthesizing CTFs with excellent photo- and electro-catalytic properties.

2 Synthesis strategies of covalent triazine frameworks

Adjustment of monomers, synthetic methods and synthetic conditions for synthesizing CTFs is of great importance for controlling the structures [23]. Of course, different synthetic methods will form CTFs with different morphologies, which play an important role in their structures. Herein, the main reported synthetic methods for CTFs are summarized and discussed.

2.1 Ionothermal synthesis

In 2008, Kuhn's team synthesized a promising new high-performance covalent triazine backbone by ionothermal dynamic trimerization reaction using a variety of inexpensive and abundant aromatic nitriles for the first time, including dicyanobenzene (DCB), 4,4-biphenyldicyano (DCBP), 2,5-dicarbonitrile thiophene (DCT), 2,6-dicyanopyridine (DCP) and 5'-(4-cyanophenyl)-[1,1,3,1-terphenyl]-4,4-dicarbonitrile (TCT), at high temperature by melting zinc chloride and employing ionic liquids as solvents and catalysts for the polymerization reaction [12]. Nitrile shows good solubility in this $ZnCl_2$ ionic melt due to strong Lewis acid-base interactions and $ZnCl_2$ is a good catalyst for the trimerization reaction, making it possible to meet all the conditions for obtaining crystalline porous polytriazines at 400 °C, which allows for the obtaining of triazinium-based materials with high regular porosity and surface area (Fig. 1(a)). By controlling a single variable of the reaction: kinetic conditions [24], temperature [25] and monomer species [26], Kuhn et al. prepared CTFs with different structures and properties. Although a promising triazine backbone material was successfully synthesized, when the $ZnCl_2$ content was high, highly porous, ordered, large surface area but

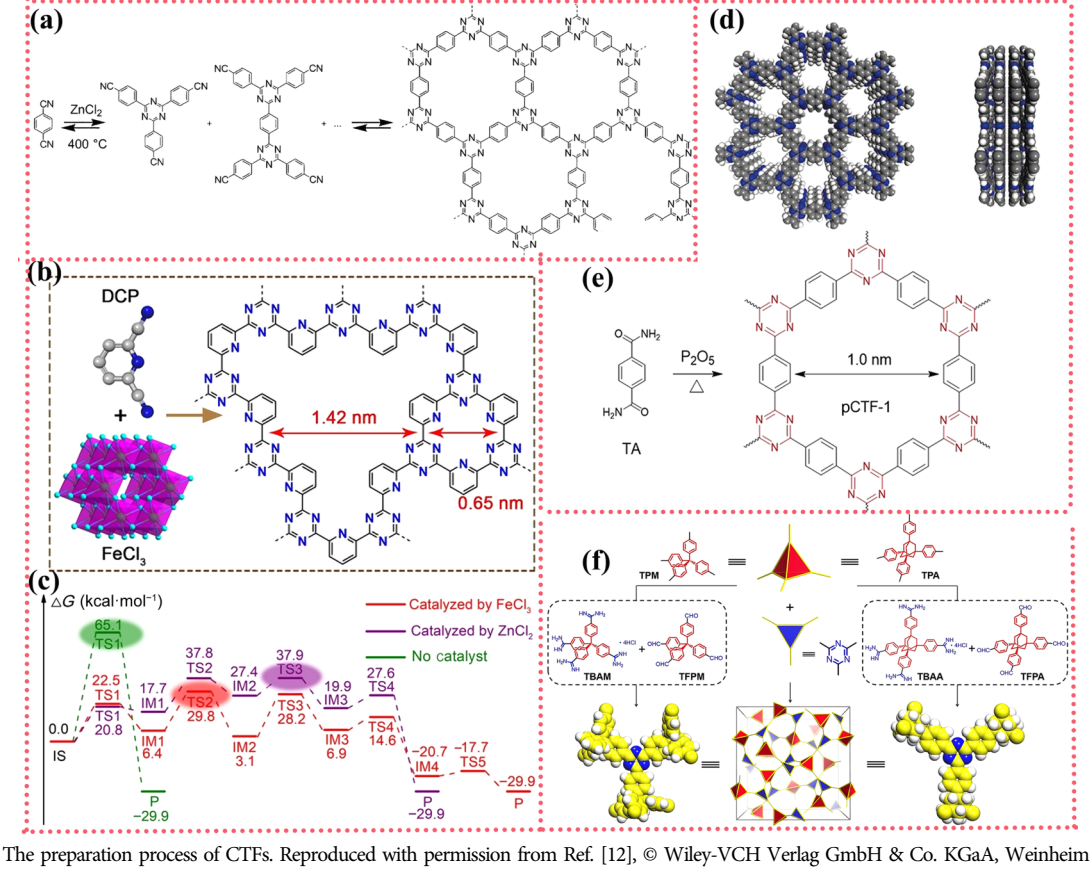

Figure 1 (a) The preparation process of CTFs. Reproduced with permission from Ref. [12], © Wiley-VCH Verlag GmbH & Co. KGaA, Weinheim 2008. (b) The preparation process of Fe-CTF. (c) DFT calculated potential energy profile for three various conditions. Reproduced with permission from Ref. [27], © Wiley-VCH GmbH 2023. (d) Space-filling diagrams of P_2O_5-catalyzed CTF-1 (pCTF-1). (e) Synthetic route of CTF-1. Reproduced with permission from Ref. [28], © Wiley-VCH Verlag GmbH & Co. KGaA, Weinheim 2018. (f) The synthesis of three-dimensional (3D) crystalline CTFs. Reproduced with permission from Ref. [29], © Wiley-VCH GmbH 2022.

amorphous materials were still produced in the reaction mixture and crystalline product was not obtained, unfortunately. Based on that, Xu et al [27] used $FeCl_3$ as a catalyst (more Lewis acidic than $ZnCl_2$, its low boiling point allowed the reaction to be carried out under very mild reaction conditions), to activate cyano and promote the catalytic polymerization of cyclo-trimer with a simple and convenient way under solvent-free conditions, and succeeded for the first time in obtaining crystalline bi-porous CTFs with a new molecular network structure and a special laminated shape (Fe-CTF) (Fig. 1(b)). Relevant control experiments were also carried out and it was found that synthesis using the $FeCl_3$ catalyst resulted in crystalline CTF catalysts, whereas both the $ZnCl_2$ catalyzed and catalyst-free routes yielded amorphous CTF products (Fig. 1(c)), which is a great improvement over the former work and points the way to the development of catalysts for the preparation of crystalline CTFs.

2.2 Phosphorus pentoxide catalytic method

In order to solve the problem of small specific surface area of the prepared CTFs, the scientists used non-metallic catalytic approaches. For example, Beak et al. [28] proposed the use of phosphorus pentoxide as a catalyst for the preparation of CTFs (Figs. 1(d) and 1(e)). Using phosphorus pentoxide to catalyze the direct condensation of aromatic amides to form triazine rings, compared with the ionothermal synthesis of CTFs using metal catalysts, the synthesis method not only retains the good crystallinity of the catalysts, but also has a large specific surface area and porosity. This preparation method gets rid of the need to remove residual metal ions and residual inorganic matter, which has been used in storage and gas adsorption. However, the synthesis temperature in the method is as high as 400 °C, and carbonation still exists during the polymerization process, resulting in the applicability of the method not being highlighted.

2.3 Polycondensation method

To address the pending issues of slow growth of the CTFs and poor reversible covalent bonding of triazine bonds, Tan et al. [29] used symmetric tetrahedral benzamidine hydrochloride and tetrahedral benzaldehyde to synthesize symmetric triangular triazine rings in the cubic carbon nitride (CTN) topology by applying a cascade condensation method via a reversible/irreversible reaction, respectively. It was connected by planar triangular rings, and two crystalline CTFs were obtained (Fig. 1(f)). In contrast to the high-temperature conditioned thermal synthesis prepared by Kuhn and colleagues at 400 °C, the condensation reaction conditions are simple and do not destroy the structure to cause partial carbonation, ensuring the internal ordered structure of the CTFs. The relatively mild conditions provide a potential methodological guide for large-scale industrial production, but with minor drawbacks such as the long reaction time.

2.4 Ultra-strong acid catalyzed method

As early as 2012, Cooper et al. [30] reported a synthetic strategy using trifluoromethanesulfonic acid (TfOH) superacid-catalyzed trimerization to synthesize semi-crystalline CTFs with a range of different colors with low specific surface area at room temperature and microwave-assisted conditions. This method solves the problem of structural carbonization at high temperatures and is more conducive to the preparation of the sheet-like crystals. To solve the significant drawbacks of the prepared catalysts such as low specific surface area and non-strong crystalline state, Dai et al. used a two-step tandem method to prepare highly crystalline CTFs using a two-step tandem method in 2020 [31]. Firstly, an ultra-strong acid-catalyzed reaction for 12 h at 250 °C, followed by a heat treatment at 350 °C under mild, no metal and solvent free conditions, which yielded highly crystalline CTFs with a specific surface area of 646 $m^2 \cdot g^{-1}$. The strategy opens a door for crystalline CTFs with tunable optoelectronic properties. However, the strong acidity of the ultra-strong acid catalysis method places high demands on the synthesis equipment.

3 The application of covalent triazine frameworks in photo- and electro-catalysis

3.1 Photocatalytic fields

CTFs possess a strong π-conjugated structure, and their triazine rings are rich in nitrogen and have high electron mobility to provide more active sites for the reaction [32, 33]. In recent years, CTFs have been applied in photocatalysis, including water splitting and CO_2 reduction reactions. Table 1 summarizes some of the catalytic performance parameters of CTFs-based photocatalysts.

3.1.1 Water splitting

Establishing appropriate insertion distances in CTFs can regulate light absorption and electronic structure, which has become a research direction for photocatalytic hydrogen evolution [44]. Chlorine (Cl) with a relatively suitable ionic radius (1.81 Å) is well

Table 1 Summary of some catalytic properties of CTF-based photocatalysts

Photocatalyst	Reaction types	Illumination range	Hydrogen production rate ($\mu mol \cdot g^{-1} \cdot h^{-1}$)	Cyclic performance	AQE	CO production rate ($\mu mol \cdot g^{-1} \cdot h^{-1}$)	References
Cl-ECF	Water splitting	$\lambda > 420$ nm	1296	16 h	—	—	[34]
CTFS-1-10	Water splitting	$\lambda > 420$ nm	4992.3	26 h	1.3%	—	[35]
CTFSe-1-10	Water splitting	$\lambda > 420$ nm	5782.8	26 h	1.7%	—	[35]
CTF-TPE@Co-3	Water splitting, CO_2 reduction	$\lambda > 420$ nm	5978	7 h	—	6616	[36]
CTF-Bpy-Co-3	Water splitting	420 nm	1503	5 h	0.233%	—	[37]
Bpy-CTF	Water splitting	$\lambda > 420$ nm	322	5 h	0.56%	—	[38]
CTF-amide-1	Water splitting	420 nm	1133	12 h	0.79%	—	[39]
Co-FPy-CON	CO_2 reduction	420 nm	—	—	—	1681	[40]
Fe_2O_3@Por-CTF10	CO_2 reduction	$\lambda > 420$ nm	—	—	—	400	[41]
FC1	CO_2 reduction	400 nm	—	96 h	0.298%	29,100	[42]
Ni (Cl)ON_3Por	CO_2 reduction	$\lambda > 420$ nm	—	—	2.73%	24,700	[43]
Ni (Cl)SN_3Por	CO_2 reduction	$\lambda > 420$ nm	—	—	4.29%	38,800	[43]

suited for insertion into layered CTFs, but the strong van der Waals force of covalent Cl^- makes its insertion into the interlayer of CTFs difficult to achieve at present. Notably, Wu and others prepared Cl-intercalated CTF-1 (Cl-ECF) photocatalysts [34] by synthesizing CTF-1 through the reported thermal oxidation method at first, and then Cl^- insertion into the interlayer channels of CTFs was easily achieved by simple ball-milling exfoliation and strong acid-assisted preparation (Fig. 2(a)). The ball milling process can easily overcome the strong covalent interlayer van der Waals forces by generating heat and mechanical shear, thus enabling stable covalent Cl^- embedding in layered CTFs by ball milling stripping in combination with the non-oxidizing acid HCl and improving its electronic structure and promoting charge transfer. The hydrogen production rate of the Cl-ECF catalyst reached 1.296 $mmol^{-1}·h^{-1}$ under visible light irradiation (Fig. 2(b)), and the stability in the catalytic reaction hardly decreased after 16 h of continuous irradiation, showing excellent photocatalytic ability (Fig. 2(c)). In addition, Li and colleagues designed a novel molecular heterojunction photocatalyst based on benzothiadiazole (BT) and thiophene (Th) doped into a covalent triazine framework for photocatalytic H_2 production [45]. The research team analyzed the optical band gap using diffuse reflection spectroscopy (DRS) and pointed out that CTFs (CTF-BT/Th) red-shifts of the absorption edge with increasing Th content, and the staggered arrangement of the band gaps allows for the opposite migration of photoexcited electrons and holes across the heterojunction (Fig. 2(d)).

This electronic structure makes it favorable for photocatalytic hydrogen production. The hybridized CFT-BT/Th exhibited a high hydrogen production rate of 6.6 $mmol·g^{-1}·h^{-1}$ and an Apparent quantum efficiency (AQE) of 7.3% at a specific 420 nm wavelength (Figs. 2(e) and 2(f)). Its excellent electrocatalytic performance mainly depends on the heterostructure can greatly improve the charge-carrier-separation efficiency (Fig. 2(g)) [46]. Wang et al. constructed related polymer photocatalysts using Th or BT units as dopant monomers similarly [47]. The density functional theory (DFT) calculation results demonstrated that the modified CTF-0.5BT and CTF-0.5Th produce significant anisotropic charge transfer behavior, which enhances the intensity of light absorption. Thus, the copolymer of this molecular unit has a great impact on improving the performance of photocatalytic hydrogen production (Figs. 2(h) and 2(i)).

3.1.2 *CO_2 reduction reactions*

Due to the abundance and high affinity of nitrogen in CTFs, attention has been directed towards utilizing it for CO_2 capture and fixation. Coskun and his colleagues synthesized charged triazine framework catalysts (cCTF) for the first time by ionothermal trimerization using violet alkene diketones as monomers [48]. By controlling the reaction temperature, it was found that cCTF-500 has richer mesoporous structure compared

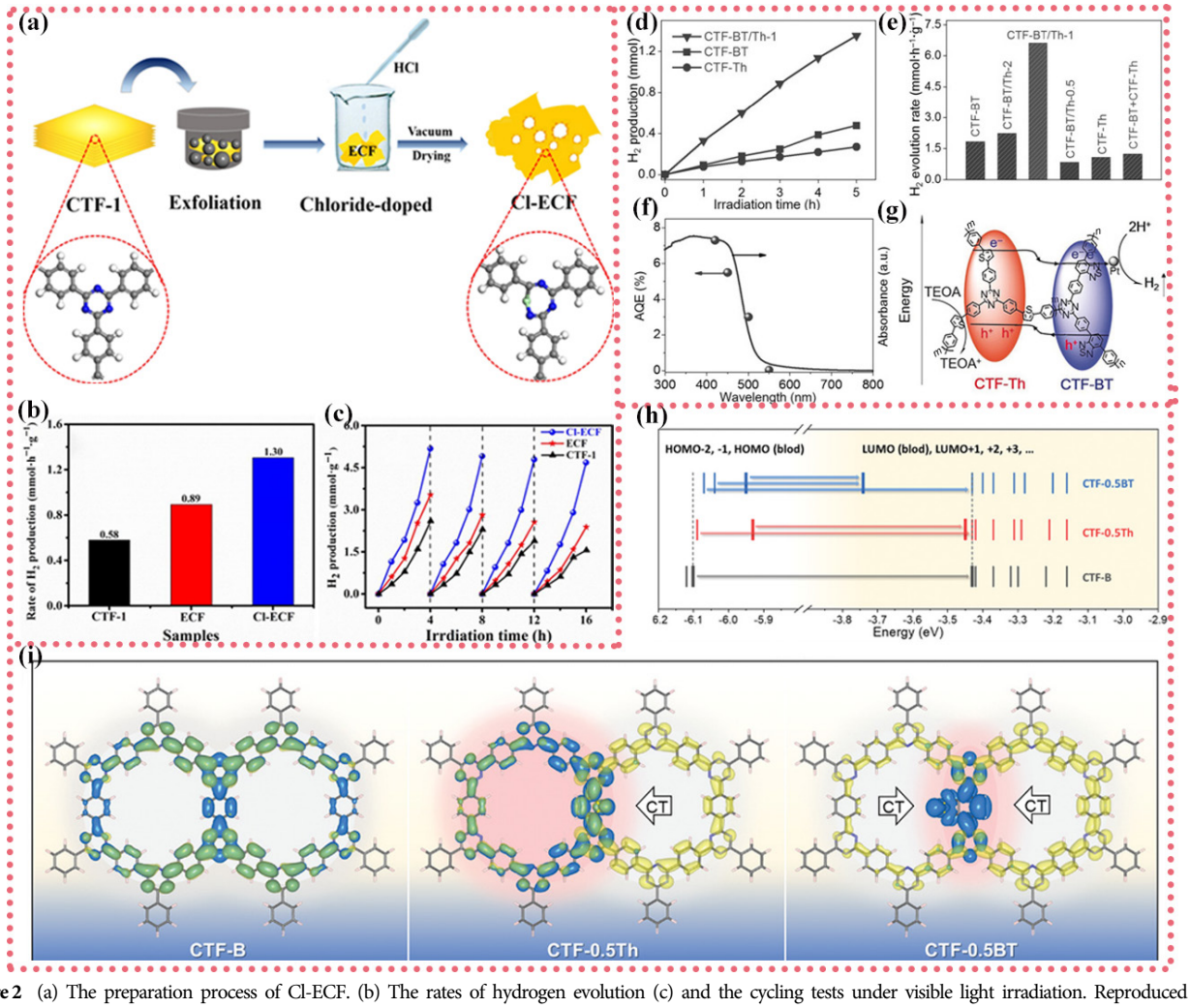

Figure 2 (a) The preparation process of Cl-ECF. (b) The rates of hydrogen evolution (c) and the cycling tests under visible light irradiation. Reproduced with permission from Ref. [34], © Elsevier B.V. 2020. (d) Photocatalytic hydrogen production capacity of different catalysts. (e) Average hydrogen-production rates. (f) Wavelength-dependent AQE. (g) Facilitated charge-carrier separation diagram. Reproduced with permission from Ref. [45], © Wiley-VCH Verlag GmbH & Co. KGaA, Weinheim 2019. DFT calculations (h) the theoretical band structures. (i) Charge density distribution of the lowest unoccupied molecular orbital (LUMO) (blue) and LUMO+1 (yellow). Reproduced with permission from Ref. [47], © Wiley-VCH GmbH 2022.

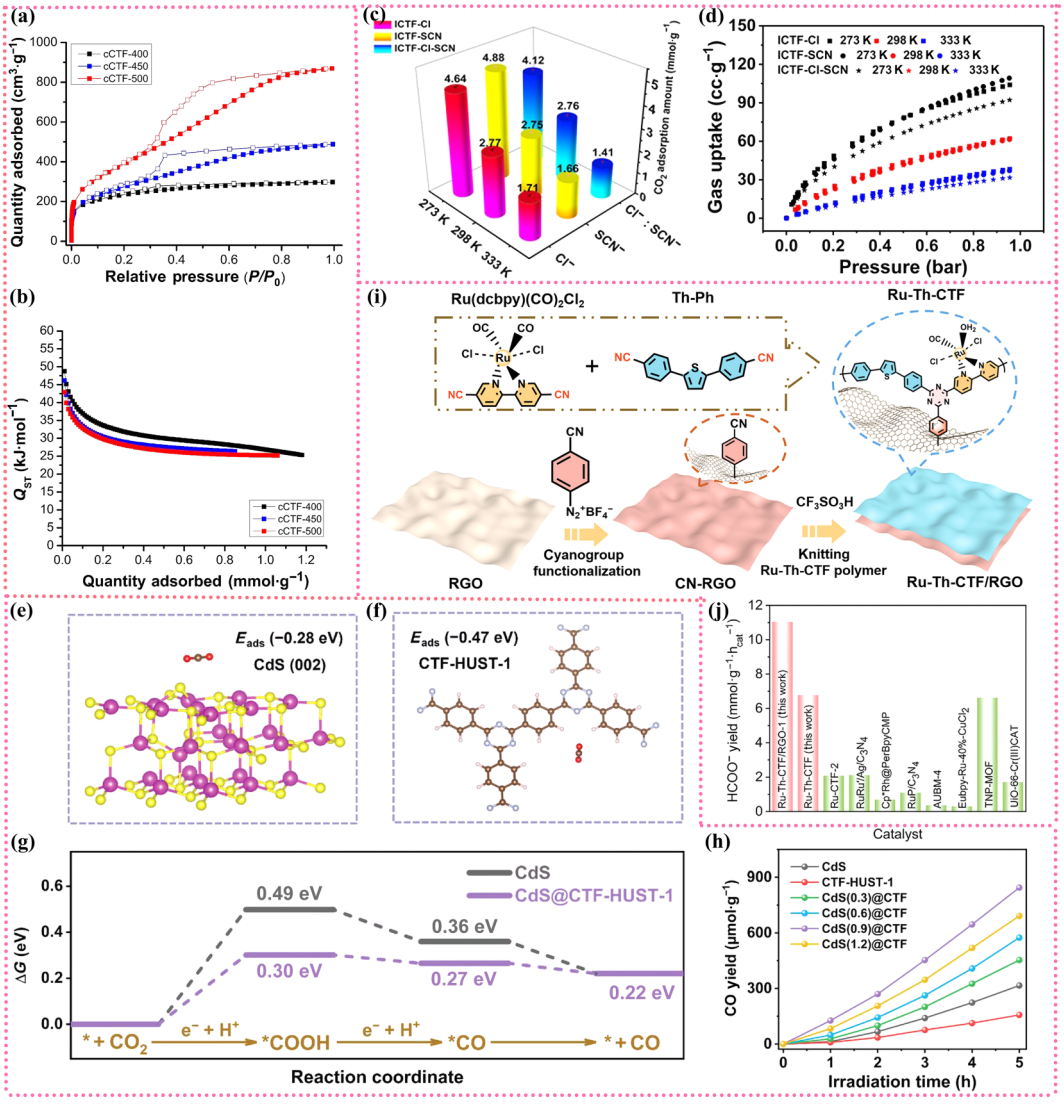

Figure 3 (a) Argon adsorption–desorption isotherms (solid line-adsorption, dash line- desorption). (b) Qst plots. Reproduced with permission from Ref. [48], © American Chemical Society 2017. ((c) and (d)) CO_2 capture capacities and adsorption isotherms at different temperatures. Reproduced with permission from Ref. [49], © American Chemical Society 2020. The adsorption energy of (e) CdS (002) and (f) CTF-HUST-1. (g) Gibbs free energy diagrams. (h) Photocatalytic properties. Reproduced with permission from Ref. [50], © Wiley-VCH GmbH 2023. (i) Flowchart for the preparation of Ru-Th-CTF/RGO. (j) Catalytic conversion rate. Reproduced with permission from Ref. [55], © Wiley-VCH GmbH 2023.

to cCTF-400 and cCTF-450 (Fig. 3(a)), which made it easier to open up the triazine ring to break covalent bonds. The multilevel network structure formed is more favorable for CO_2 conversion. It shows significant heat of CO_2 adsorption (43 kJ·mol^{-1}) and affinity also up to 133 mg·g^{-1} (1 bar) at zero coverage (Fig. 3(b)). The study provides a new way to fix CO_2 by conversion of charged porous organic polymers. Wang et al. also constructed a bipyridine-based ionic CTF catalyst (ICTF) using ionothermal polymerization reactions [49]. By freely adjustable exchange of the anion Cl^- and 1,1'-bis(cyanomethyl)-[4,4'-bipyridine]-1,1'-diium thiocyanate (IL-SCN) increases the specific surface area and affinity for gases, which was found to be more than 1 bar for the ability of catalysts to capture CO_2 at different temperatures (Fig. 3(c)). Meanwhile, higher CO_2 uptake was observed for ICTF-Cl compared to ICTF-SCN (Fig. 3(d)), which was attributed to the high nucleophilicity of Cl^-. Chen groups produced heterojunction photocatalysts of CdS@CTF-HUST-1 (HUST = Huazhong University of Science and Technology) with core–shell structure for CO_2 reduction by combining CFT with cadmium sulfide nanospheres through the introduction of amino groups in the coating of CdS nanospheres [50]. It was shown that the catalyst has a high CO yield rate of 168.77 μmol·g^{-1}·h^{-1} and all the heterojunction catalysts exhibit better photocatalytic performance than the individual heterojunction catalysts (Fig. 3(h)). The adsorption energy of CTF-HUST-1-0.47 eV is lower than the adsorption energy of the (002) crystalline surface of CdS-0.28 eV alone by DFT calculations (Figs. 3(e) and 3(f)), and the core–shell structure can improve the strength of CO_2 adsorption [51–53]. As shown by the Gibbs free energy diagram (Fig. 3(g)), the heterojunction structure can effectively reduce the reaction energy potential during the CO_2 reduction process [54], which is also an important reason for optimizing the CO_2 adsorption conversion. Low charge separation efficiency and difficult charge transfer resistance are large impediments to the low efficiency of the catalytic conversion of carbon dioxide. In order to solve this problem, Fan's group [55] prepared a Schottky heterojunction catalyst (Ru-Th-CTF/reduced graphene oxide (RGO)) with a large π-domain and π-stacking for photocatalytic reduction of CO_2 to formate (Fig. 3(i)). The main method was *in situ* growth of the multicascade donor acceptor structure D–A1–A2 system (Ru-Th-CTF) onto the surface of reduced graphene oxide by bonding cooperation and π–π stacking. The synergistic effect of the heterojunction with the system allows for effective charge separation and transport in the lateral separation as well as in the vertical separation [56]. The unit-site Ru unit in the heterojunction catalyst Ru-Th-CTF/RGO is an effective secondary electron acceptor for multilevel charge

separation/transport in the transverse direction, which efficiently separates and modulates the energy band positions. In addition, graphene stacked by bonding cooperation is regarded as a hole-extraction layer, and its enhanced π–π stacking ability constructs favorable charge migration π-delocalized channels. The photogenerated electrons can be fully utilized for the relevant reduction reactions to accelerate the separation/transport of photogenerated charges in the vertical direction of the catalyst. The construction of an efficient charge transfer pathway in CTFs for the oriented transport of photoexcited electrons resulted in an unprecedented catalytic conversion of 11,050 μmol·g^{-1}·h^{-1} (Fig. 3(j)), highlighting the importance of the Schottky and D–A1–A2 systems for CO_2 reduction.

In some other studies, deposition-anchored Co, Cu single atoms embedded in CTFs [57, 58], bipyridine-based CTFs introduced with single-dot cobalt (CTF-Bpy-Co) [59], boron-doped CTFs [60], perfluorinated CTFs [61], crystalline CTFs nanosheets [62, 63] and photo-deposition enabled Pt single-atom-anchored CTFs [64] have also been widely used in the field of photocatalysis for water splitting and CO_2 reduction. In the field of improving the photocatalytic performance of catalysts, wide visible light absorption range, suitable energy band structure, and high photocurrent density are undoubtedly important. Of course, the high specific surface area and rich pore structure of the materials also help to enhance their catalytic activity. The catalytic mechanism needs to be deeply investigated to improve the catalyst activity, stability and production selectivity in order to meet the demand, which indicates certain research directions for the future work.

3.2 Electrocatalytic fields

CTFs have a unique structure with a high nitrogen content in their triazine rings, and their open pore structure and large specific surface area have attracted extensive attention in the field of electrocatalysis. To address the problems of poor catalyst conductivity due to low nitrogen content, the researchers conducted a series of studies on CTF-based heteroatom-doped materials and CTF-based carbon materials, which effectively promoted charge and ion transfer within the catalysts and increased the relevant electrocatalytic properties. Table 2 summarizes some of the catalytic performance parameters of CTFs-based electrocatalysts.

Fan et al. prepared Fe/N/S/C electrocatalysts based on CTF derivatives using six aromatic nitriles [75]. The high ratio of nitrile groups to benzene rings in CTF precursors could form more N-doped micropores and increase the reactive active sites of Fe-N_x. At the same time, the S doping centered the Fe/N/C catalysts and increased the reactive active sites, which resulted in the improvement of oxygen reduction reaction (ORR) performance (Fig. 4(a)). Zhang et al. [76] proposed a metal-free catalyst material formed *in situ* by thermal initiation of the CTFs using no template. A hollow mesoporous carbon spheres (N/S-HMCS) material with rich mesoporous structure was obtained. When the heteroatom-doped nitrogen and sulfur contents were 6.1 at.% and 1.3 at.%, N/S-HMCS900 exhibited excellent ORR performance near 20% Pt/C (Fig. 4(b)). The excellent structural properties gave the material excellent performance in zinc-air batteries, and the specific capacity of the batteries exceeded 800 mAh·g^{-1} (Fig. 4(c)). Jena and co-workers [77] reported a metal-free covalent triazine skeleton electrocatalyst based on phosphorus references to produce phosphorus CTFs (PCTFs) for water splitting reaction by using hexakis-(4-cyanophenyloxy)cyclotriphosphazenes (P-CN) as the raw material and adjusts different synthesis conditions (temperature and $ZnCl_2$ content) of the relevant ionic heat (Fig. 4(d)). The linear sweep voltammetry (LSV) curves showed that the reduction current increased of PCTF-10500 ($ZnCl_2$ content of 10 equiv and reaction temperature of 500 °C), the hydrogen evolution was high when the sweep rate was 20 mV·s^{-1} (Fig. 4(e)).

The presence of the heteroatom P generates a high electron density on the carbon atom, forming more site defects and greatly improving the catalytic performance, as shown by the relevant free energy calculation. Wang et al. utilized the synthesized nanotubular CTFs as the precursor [78], via one-pot hydrothermal and metal-organic framework (MOF) doping, obtained noble metal-free CTF@MOF-*x* (*x* = 15 wt.%, 24 wt.% and 33 wt.%) catalysts for the first time. The obtained MC-24-700 catalyst by carbonization can achieve ORR catalytic performance of 0.770 V under alkaline conditions, which is slightly less than commercial Pt/C. The greatest benefit of this report is to provide a new CTF-MOF doped catalysts, which makes it difficult for CTF to collapse and aggregate during pyrolysis, and thus the catalytic activity can be greatly improved. All of these literature reports favor the preparation of doped materials and thus promote the electrocatalytic performance, and very few reports tend to prepare crystalline CTFs, because the development of the crystalline CTF technology method is not so mature. Recently, Xu and his groups synthesized crystalline layered bi-porous Fe-CTF catalysts using ferric chloride-catalyzed polymerization of 2,6-pyridine dihydropyridine (DCP) for the first time [27]. The experiments were carried out under solvent-free conditions, followed by ball-milling stripping to obtain few-layer crystalline nanosheets (Fe-CTF NSs) simply (Fig. 4(f)). The unique Fe-N_3 structure enables it to exhibit significant ORR catalytic activity ($E_{1/2}$ = 0.902 V), excellent zinc-air battery performance (specific capacity of

Table 2 Summary of some catalytic properties of CTF-based electrocatalysts

Electrocatalyst	Reaction types	Battery electrolyte	Overpotential (J = 10 mA·cm^{-2})	$E_{1/2}$ (V vs. RHE[a])	Power density (mW·cm^{-2})	Cycling stability (h)	References
HNPC-900	ORR	6 M KOH + 0.2 M $Zn(OAc)_2$	—	0.85	120	380	[65]
ACTF-α-900	ORR	6 M KOH	—	0.86	651	80	[66]
NPF-CNF-800	OER, ORR	6 M KOH + 0.2 M $Zn(OAc)_2$	330 mV	0.85	159	120	[67]
ACTP-2	ORR	6 M KOH + 0.2 M $Zn(OAc)_2$	—	0.80	190	35	[68]
SP-NC	ORR	6 M KOH	—	0.87	209	20	[69]
N-HCNFs	OER, ORR	6 M KOH + 0.2 M $Zn(OAc)_2$	243 mV	0.84	170	70	[70]
NPF-CNS	OER, ORR	6 M KOH + 0.2 M $Zn(OAc)_2$	340 mV	0.81	144	125	[71]
Fe-TTF-800	OER, ORR	6 M KOH + 0.2 M $Zn(OAc)_2$	154 mV	0.891	214.2	550	[72]
Co-NTMCs@NSC	OER, ORR	6 M KOH + 0.2 M $Zn(OAc)_2$	284 mV	0.833	262	—	[73]
FeNi-CNC-800	OER, ORR	6 M KOH + 0.2 M $Zn(OAc)_2$	320 mV	0.840	115	250	[74]

[a]RHE: reversible hydrogen electrode.

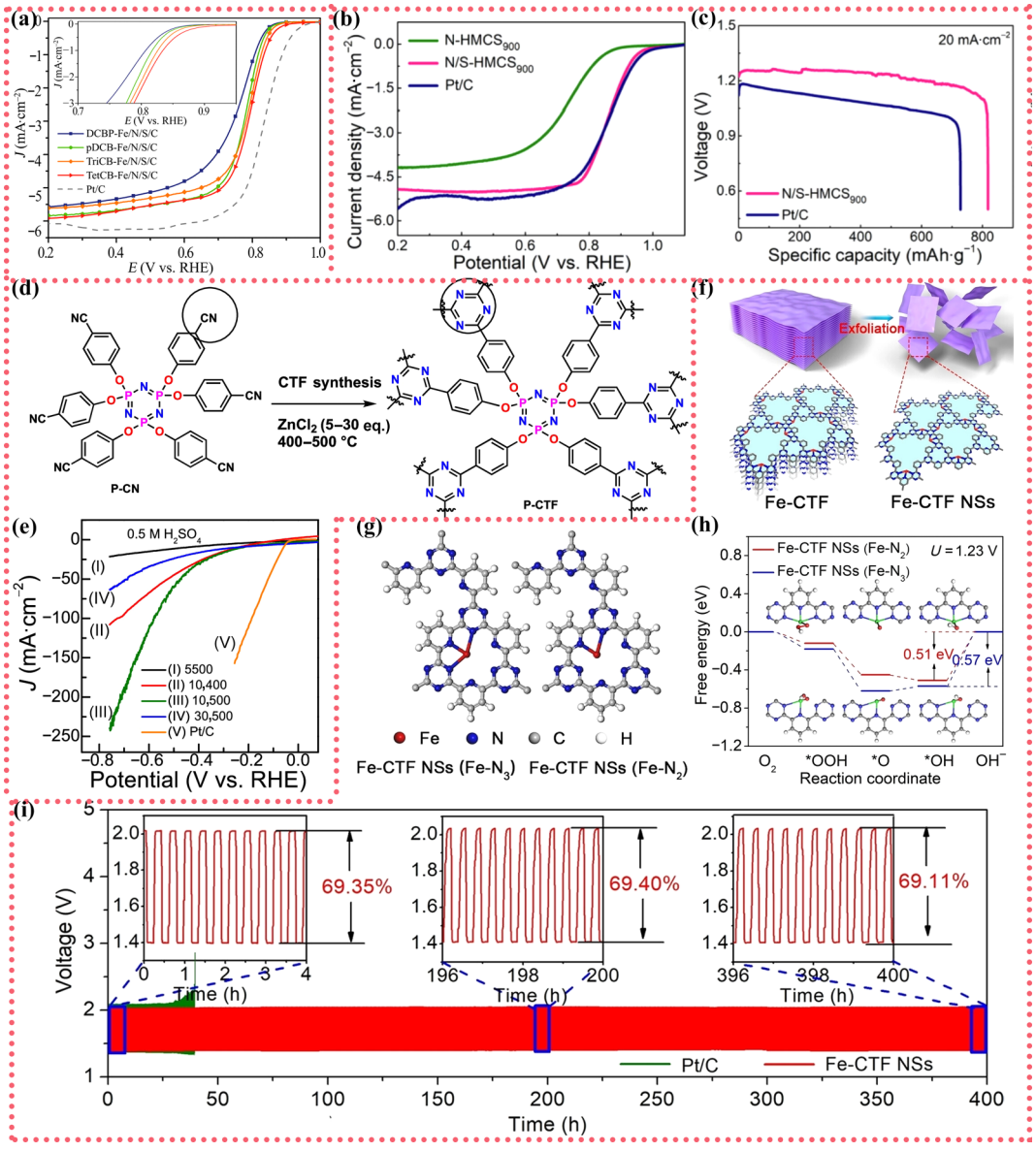

Figure 4 (a) ORR polarization curves. Reproduced with permission from Ref. [75], © Wiley-VCH Verlag GmbH & Co. KGaA, Weinheim 2018. (b) LSV curves of various materials. (c) Discharge curves of Zn-air batteries. Reproduced with permission from Ref. [76], © Elsevier Inc. 2021. (d) Synthesis process of P-CTF. (e) LSV curves at 20 mV·s^{-1}. Reproduced with permission from Ref. [77], © American Chemical Society 2023. (f) The preparation of Fe-CTF NSs. (g) Structural models of Fe-N_3 and Fe-N_2. (h) Gibbs free energy diagrams at U = 1.23 V. (i) Long cycle stability curves. Reproduced with permission from Ref. [27], © Wiley-VCH GmbH 2023.

811 mAh·g^{-1}, power density of 230 mW·cm^{-2}) and superior long cycle stability (Fig. 4(i)). X-ray absorption spectroscopy and DFT calculations reveal the dynamic evolution of Fe-N_3 to Fe-N_2, and the conversion step of Fe-N_2 from *OH to OH^- requires a small reaction energy barrier (0.51 eV) (Figs. 4(g) and 4(h)), which is one of the reasons why the electrocatalytic reaction works so well.

In addition, Voort et al. [79] synthesized tailored CTF networks with strong oxidation using hexaazatriphenylenes (HAT) as a monomer, showing high H_2O_2 yield. Ye et al. used self-doped pyrolysis to encapsulate amorphous MnO_2 sheets into CTFs to obtain A-MnO_2/NSPC carbon spheres for ORR/oxygen evolution reaction (OER) bifunctional catalysis [80]. These research methods are simple and readily available, but few crystalline-based CTF catalyst materials have been reported. Moreover, the preparation of crystalline CTFs and their application in electrocatalysis is still a considerable challenge that requires continuous efforts from researchers.

4 Summary and outlook

In conclusion, for the rich pore structures, large specific surface area and excellent semiconductivity of special CTFs, it has found great applications in acting as a sensor in gas adsorption/separation, efficient energy storage, photo- and electro-catalysis in recent years. So far, the classical synthetic methods for the preparation of CTFs are mainly: ionothermal synthesis, phosphorus pentoxide-catalyzed method, polycondensation method and ultra-strong acid-catalyzed method. Although the synthesis methods of CTFs have been improved, the synthesis of CTFs in the crystalline state is still very limited. Certainly, CTFs have made some achievements in the field of photo- and electro-catalysis, but there are still some challenges to be solved. In order to design high-performance materials for functional CTFs, some points are made below:

(1) Highly crystalline state of CTFs. Most of the prepared CTFs are non-crystalline, however, high crystallinity facilitates charge separation and transfer, which can lead to highly tunable molecular structure and porosity, increase the active sites for catalytic reactions, and the catalytic activity of such crystalline carriers will be more superior compared to amorphous CTFs. Constructing hydrogen bonds and assembling crystalline frameworks all provide research ideas for crystallized CTFs.

Therefore, obtaining crystallized CTFs under suitable and simple reaction conditions still requires a great deal of exploration and research.

(2) Avoid severe carbonization. It is known from the synthesis method of CTFs, like phosphorus pentoxide catalyzed method such synthesis method is the same. The use of high reaction temperatures in synthesis will cause severe carbonization during polymerization, resulting in a certain collapse of the structure and causing certain defective structures, thus destroying the ordered structure, which is not conducive to the production of excellent catalytic effects in photo- and electro-catalysis. Therefore, to make the carbonation not so severe and to increase the catalytic effect, it is necessary to choose the appropriate synthesis temperature and to allow the reaction to proceed in a fast and orderly manner.

(3) Large-scale production. Although the preparation of CTFs has been widely studied, most of the research methods do not meet the requirements of large-scale production in terms of reaction temperature, reaction conditions, and reaction time, which forces us to pay attention to the issue of yield for large-scale production.

(4) Reaction mechanisms. In-depth investigation of the reaction mechanism of the CTFs in photo- and electro-catalysis by *in situ* characterization and DFT calculations. By understanding the structure–function connectivity between active structures and catalytic behaviors for the CTFs and deepening their structure–function related property relationships have significant values in influencing the design of high-performance CTFs-based catalysts.

(5) Future applications in catalysis. The tailored optical and semiconductive properties of the CTFs make them promising metal-free polymeric photocatalysts. Meanwhile, the low skeletal density and large specific surface area structure of the CTFs provide channels for good hydrogen storage, which provides theoretical guidance for the design of excellent CTFs-based photocatalysts. In addition, the abundant nitrogen content in the structure of the CTFs and the good porosity make them widely used in the electrocatalytic field. In the process of future development, constructing the CTFs-based catalysts with conductive materials such as carbon nanotubes, graphene oxide, and carbon quantum dots is an effective method to improve the electrocatalytic conductivity of the CTFs, which leads to a wide range of applications for CTFs-based catalysts in the catalysis and energy storage materials areas.

Although CTFs have made great progress in photo- and electro-catalysis, there are still significant limitations in producing economically viable, high activity and high crystalline state catalysts. The further evolvement of photo- and electro-catalytic monomers based on CTFs have the ideal potential to be candidate catalysts for rapid sustainable and stable development of photo- and electro-catalysis.

Acknowledgements

We gratefully acknowledge the National Natural Science Foundation of China (Nos. 42167068 and 22269020), Gansu Province Higher Education Industry Support Plan Project (No. 2023CYZC-68), and the Hubei Province Outstanding Youth Fund Project (No. 2023AFA108).

References

[1] Qian, Z. F.; Wang, Z. J.; Zhang, K. A. I. Covalent triazine frameworks as emerging heterogeneous photocatalysts. *Chem. Mater.* **2021**, *33*, 1909–1926.

[2] Liu, M. Y.; Guo, L. P.; Jin, S. B.; Tan, B. E. Covalent triazine frameworks: Synthesis and applications. *J. Mater. Chem. A* **2019**, *7*, 5153–5172.

[3] Sun, R. X.; Tan, B. E. Covalent triazine frameworks (CTFs): Synthesis, crystallization, and photocatalytic water splitting. *Chem.—Eur. J.* **2023**, *29*, e202203077.

[4] Haldar, S.; Waentig, A. L.; Ramuglia, A. R.; Bhauriyal, P.; Khan, A. H.; Pastoetter, D. L.; Isaacs, M. A.; De, A.; Brunner, E.; Wang, M. C. et al. Covalent trapping of cyclic-polysulfides in perfluorinated vinylene-linked frameworks for designing lithium-organosulfide batteries. *ACS Energy Lett.* **2023**, *8*, 5098–5106.

[5] Shao, J. L.; Zhou, Z. F.; Chen, X.; Tian, R. Y.; Zhang, Z. H.; Li, G. C. Pseudo-covalent triazine frameworks for superior Li-S batteries. *Chem. Eng. J.* **2024**, *481*, 148209.

[6] Wu, Y. A.; McNulty, I.; Liu, C.; Lau, K. C.; Liu, Q.; Paulikas, A. P.; Sun, C. J.; Cai, Z. H.; Guest, J. R.; Ren, Y. et al. Facet-dependent active sites of a single Cu_2O particle photocatalyst for CO_2 reduction to methanol. *Nat. Energy* **2019**, *4*, 957–968.

[7] Liu, G.; Liu, S. B.; Lai, C.; Qin, L.; Zhang, M. M.; Li, Y. X.; Xu, M. Y.; Ma, D. S.; Xu, F. H.; Liu, S. Y. et al. Strategies for enhancing the photocatalytic and electrocatalytic efficiency of covalent triazine frameworks for CO_2 reduction. *Small*, in press, DOI: 10.1002/smll.202307853.

[8] Li, Y. X.; Lai, C.; Liu, S. B.; Fu, Y. K.; Qin, L.; Xu, M. Y.; Ma, D. S.; Zhou, X. R.; Xu. F. H.; Liu, H. D. et al. Metallic active-site engineering: A bridge between covalent triazine frameworks and high-performance catalysts. *J. Mater. Chem. A* **2023**, *11*, 2070–2091.

[9] Yang, S.; Gao, Z.; Hu, Z. Y.; Pan, C. Y.; Yuan, J. Y.; Tam, K. C.; Liu, Y. N.; Yu, G. P.; Tang, J. T. Regulating the tautomerization in covalent organic frameworks for efficient sacrificial agent-free photocatalytic H_2O_2 production. *Macromolecules* **2024**, *57*, 2039–2047.

[10] Niu, Q.; Mi, L. H.; Chen, W.; Li, Q. J.; Zhong, S. H.; Yu, Y.; Li, L. Y. Review of covalent organic frameworks for single‐site photocatalysis and electrocatalysis. *Chin. J. Catal.* **2023**, *50*, 45–82.

[11] Xing, Z. P.; Zhang, J. Q.; Cui, J. Y.; Yin, J. W.; Zhao, T. Y.; Kuang, J. Y.; Xiu, Z. Y.; Wan, N.; Zhou, W. Recent advances in floating TiO_2-based photocatalysts for environmental application. *Appl. Catal. B: Envrion. Energy* **2018**, *225*, 452–467.

[12] Kuhn, P.; Antonietti, M.; Thomas, A. Porous, covalent triazine-based frameworks prepared by ionothermal synthesis. *Angew. Chem., Int. Ed.* **2008**, *47*, 3450–3453.

[13] Abednatanzi, S.; Derakhshandeh, P. G.; Tack, P.; Muniz-Miranda, F.; Liu, Y. Y.; Everaert, J.; Meledina, M.; Bussche, F. V.; Vincze, L.; Stevens, C. V. et al. Elucidating the promotional effect of a covalent triazine framework in aerobic oxidation. *Appl. Catal. B: Envrion. Energy* **2020**, *269*, 118769.

[14] Zhen, J. H.; Shen, J. C.; Sun, T.; Wang, C. X.; Lyu, P. B.; Xu, Y. X. Direct synthesis of ultrathin crystalline two-dimensional triazine polymers from aldoximes. *CCS Chem.* **2024**, *6*, 932–940.

[15] Liang, Z. Z.; Shen, R. C.; Ng, Y. H.; Fu, Y.; Ma, T. Y.; Zhang, P.; Li, Y. J.; Li, X. Covalent organic frameworks: Fundamentals, mechanisms, modification, and applications in photocatalysis. *Chem Catal.* **2022**, *2*, 2157–2228.

[16] Hasija, V.; Patial, S.; Raizada, P.; Khan, A. A. P.; Asiri, A. M.; Van Le, Q.; Nguyen, V. H.; Singh, P. Covalent organic frameworks promoted single metal atom catalysis: Strategies and applications. *Coord. Chem. Rev.* **2022**, *452*, 214298.

[17] Liu, S. S.; Wang, M. F.; He, Y. Z.; Cheng, Q. Y.; Qian, T.; Yan, C. L. Covalent organic frameworks towards photocatalytic applications: Design principles, achievements, and opportunities. *Coord. Chem. Rev.* **2023**, *475*, 214882.

[18] Xiang, Z. H.; Cao, D. P.; Huang, L.; Shui, J. L.; Wang, M.; Dai, L. M. Nitrogen-doped holey graphitic carbon from 2D covalent organic polymers for oxygen reduction. *Adv. Mater.* **2014**, *26*, 3315–3320.

[19] Nowsheenah, F.; Abu, T.; Athar, A. H. Facile synthesis of a nitrogen-rich covalent organic framework for the efficient capture of iodine. *J. Mater. Chem. A* **2024**, *12*, 10539–10553.

[20] Patial, S.; Soni, V.; Kumar, A.; Raizada, P.; Ahamad, T.; Pham, X. M.; Le, Q. V.; Nguyen, V. H.; Thakur, S.; Singh, P. Rational design, structure properties, and synthesis strategies of dual-pore covalent

organic frameworks (COFs) for potent applications: A review. *Environ. Res.* **2023**, *218*, 114982.
[21] Dong, B.; Wang, D. Y.; Wang, W. J. Post-functionalization of hydroxyl-appended covalent triazine framework via borrowing hydrogen strategy for effective CO_2 capture. *Micropor. Mesopor. Mat.* **2020**, *292*, 109765.
[22] Liu, Y. B.; Wu, H.; Wang, Q. Strategies to improve the photocatalytic performance of covalent triazine frameworks. *J. Mater. Chem. A* **2023**, *11*, 21470–21497.
[23] Liao, L. F.; Li, M. Y.; Yin, Y. L.; Chen, J.; Zhong, Q. T.; Du, R. X.; Liu, S. L.; He, Y. M.; Fu, W. J.; Zeng, F. Advances in the synthesis of covalent triazine frameworks. *ACS Omega* **2023**, *8*, 4527–4542.
[24] Kuhn, P.; Forget, A.; Hartmann, J.; Thomas, A.; Antonietti, M. Template-free tuning of nanopores in carbonaceous polymers through ionothermal synthesis. *Adv. Mater.* **2009**, *21*, 897–901.
[25] Kuhn, P.; Forget, A.; Su, D. S.; Thomas, A.; Antonietti, M. From microporous regular frameworks to mesoporous materials with ultrahigh surface area: Dynamic reorganization of porous polymer networks. *J. Am. Chem. Soc.* **2008**, *130*, 13333–13337.
[26] Kuhn, P.; Thomas, A.; Antonietti, M. Toward tailorable porous organic polymer networks: A high-temperature dynamic polymerization scheme based on aromatic nitriles. *Macromolecules* **2009**, *42*, 319–326.
[27] Cui, K.; Tang, X. L.; Xu, X. P.; Kou, M. C.; Lyu, P. B.; Xu, Y. X. Crystalline dual-porous covalent triazine frameworks as a new platform for efficient electrocatalysis. *Angew. Chem., Int. Ed.* **2024**, *63*, e202317664.
[28] Yu, S. Y.; Mahmood, J.; Noh, H. J.; Seo, J. M.; Jung, S. M.; Shin, S. H.; Im, Y. K.; Jeon, I. Y.; Baek, J. B. Direct synthesis of a covalent triazine-based framework from aromatic amides. *Angew. Chem., Int. Ed.* **2018**, *57*, 8438–8442.
[29] Sun, R. X.; Wang, X. Y.; Wang, X. P.; Tan, B. Three-dimensional crystalline covalent triazine frameworks via a polycondensation approach. *Angew. Chem., Int. Ed.* **2022**, *61*, e202117668.
[30] Ren, S. J.; Bojdys, M. J.; Dawson, R.; Laybourn, A.; Khimyak, Y. Z.; Adams, D. J.; Cooper, A. I. Porous, fluorescent, covalent triazine-based frameworks via room-temperature and microwave-assisted synthesis. *Adv. Mater.* **2012**, *24*, 2357–2361.
[31] Yang, Z. Z.; Chen, H.; Wang, S.; Guo, W.; Wang, T.; Suo, X.; Jiang, D. E.; Zhu, X.; Popovs, I.; Dai, S. Transformation strategy for highly crystalline covalent triazine frameworks: From staggered AB to eclipsed AA stacking. *J. Am. Chem. Soc.* **2020**, *142*, 6856–6860.
[32] Xiao, L. Y.; Qi, L. L.; Sun, J. R.; Husile, A.; Zhang, S. Y.; Wang, Z. L.; Guan, J. Q. Structural regulation of covalent organic frameworks for advanced electrocatalysis. *Nano Energy* **2024**, *120*, 109155.
[33] Qi, G. D.; Ba, D.; Zhang, Y. J.; Jiang, X. Q.; Chen, Z. H.; Yang, M. M.; Cao, J. M.; Dong, W. W.; Zhao, J.; Li, D. S. et al. Constructing an asymmetric covalent triazine framework to boost the efficiency and selectivity of visible-light-driven CO_2 photoreduction. *Adv. Sci.*, in press, DOI: 10.1002/advs.202402645.
[34] Li, S.; Wu, M. F.; Guo, T.; Zheng, L. L.; Wang, D. K.; Mu, Y.; Xing, Q. J.; Zou, J. P. Chlorine-mediated photocatalytic hydrogen production based on triazine covalent organic framework. *Appl. Catal. B: Environ.* **2020**, *272*, 118989.
[35] Chen, M. H.; Xiong, J.; Li, X. Y.; Shi, Q.; Li, T.; Feng, Y. Q.; Zhang, B. *In-situ* doping strategy for improving the photocatalytic hydrogen evolution performance of covalent triazine frameworks. *Sci. China Chem.* **2023**, *66*, 2363–2370
[36] Jana, A.; Maity, A.; Sarkar, A.; Show, B.; Bhobe, P. A.; Bhunia, A. Single-site cobalt catalyst embedded in a covalent triazine-based framework (CTF) for photocatalytic CO_2 reduction. *J. Mater. Chem. A* **2024**, *12*, 5244–5253.
[37] Sun, R. X.; Hu, X. L.; Shu, C.; Zheng, L. R.; Wang, S. Y.; Wang, X. Y.; Tan, B. E. Anchoring single Co sites on bipyridine-based covalent triazine framework for efficient photocatalytic oxygen evolution. *Chin. J. Catal.* **2023**, *55*, 159–170.
[38] Chen, H. M.; Gardner, A. M.; Lin, G. A.; Zhao, W.; Bahri, M.; Browning, N. D.; Sprick, R. S.; Li, X. B.; Xu, X. X.; Cooper, A. I. Covalent triazine-based frameworks with cobalt-loading for visible light-driven photocatalytic water oxidation. *Catal. Sci. Technol.* **2022**, *12*, 5442–5452.
[39] Li, Z. L.; Li, T. C.; Miao, J. M.; Zhao, C. X.; Jing, Y.; Han, F. Y.; Zhang, K.; Yang, X. F. Amide-functionalized covalent triazine framework for enhanced photocatalytic hydrogen evolution. *Sci. China Mater.* **2023**, *66*, 2290–2298.
[40] Wang, X. Y.; Fu, Z. W.; Zheng, L. R.; Zhao, C. X.; Wang, X.; Chong, S. Y.; McBride, F.; Raval, R.; Bilton, M.; Liu, L. J. et al. Covalent organic framework nanosheets embedding single cobalt sites for photocatalytic reduction of carbon dioxide. *Chem. Mater.* **2020**, *32*, 9107–9114.
[41] Zhang, S. Q.; Wang, S. Y.; Guo, L. P.; Chen, H.; Tan, B. E.; Jin, S. B. An artificial photosynthesis system comprising a covalent triazine framework as an electron relay facilitator for photochemical carbon dioxide reduction. *J. Mater. Chem. C* **2020**, *8*, 192–200.
[42] Kosugi, K.; Akatsuka, C.; Iwami, H.; Kondo, M.; Masaoka, S. Iron-complex-based supramolecular framework catalyst for visible-light-driven CO_2 reduction. *J. Am. Chem. Soc.* **2023**, *145*, 10451–10457.
[43] Zhong, Y. H.; Wang, Y.; Zhao, S. Y.; Xie, Z. X.; Chung, L. H.; Liao, W. M.; Yu, L.; Wong, W. Y.; He, J. Regulating the electronic configuration of Ni sites by breaking symmetry of Ni-porphyrin to facilitate CO_2 photocatalytic reduction. *Adv. Funct. Mater.*, in press, DOI: 10.1002/adfm.202316199.
[44] Sun, R. X.; Tan, B. E. Covalent triazine frameworks (CTFs) for photocatalytic applications. *Chem. Res. Chin. Univ.* **2022**, *38*, 310–324.
[45] Huang, W.; He, Q.; Hu, Y. P.; Li, Y. G. Molecular heterostructures of covalent triazine frameworks for enhanced photocatalytic hydrogen production. *Angew. Chem., Int. Ed.* **2019**, *58*, 8676–8680.
[46] Zhao, Y. X.; Chang, C.; Teng, F.; Zhao, Y. F.; Chen, G. B.; Shi, R.; Waterhouse, G. I. N.; Huang, W. F.; Zhang, T. R. Defect-engineered ultrathin δ-MnO_2 nanosheet arrays as bifunctional electrodes for efficient overall water splitting. *Adv. Energy Mater.* **2017**, *7*, 1700005.
[47] Lan, Z. A.; Chi, X.; Wu, M.; Zhang, X. R.; Chen, X.; Zhang, G. G.; Wang, X. C. Molecular design of covalent triazine frameworks with anisotropic charge migration for photocatalytic hydrogen production. *Small* **2022**, *18*, 2200129.
[48] Buyukcakir, O.; Je, S. H.; Talapaneni, S. N.; Kim, D.; Coskun, A. Charged covalent triazine frameworks for CO_2 capture and conversion. *ACS Appl. Mater. Interfaces* **2017**, *9*, 7209–7216.
[49] Zhu, H.; Lin, W. J.; Li, Q.; Hu, Y.; Guo, S. Y.; Wang, C. M.; Yan, F. Bipyridinium-based ionic covalent triazine frameworks for CO_2, SO_2, and NO capture. *ACS Appl. Mater. Interfaces* **2020**, *12*, 8614–8621.
[50] Zhang, G. P.; Li, X. X.; Chen, D. Y.; Li, N. J.; Xu, Q. F.; Li, H.; Lu, J. M. Internal electric field and adsorption effect synergistically boost carbon dioxide conversion on cadmium sulfide@covalent triazine frameworks core–shell photocatalyst. *Adv. Funct. Mater.* **2023**, *33*, 2308553.
[51] Meng, A. Y.; Cheng, B.; Tan, H. Y.; Fan, J. J.; Su, C. L.; Yu, J. G. TiO_2/polydopamine S-scheme heterojunction photocatalyst with enhanced CO_2-reduction selectivity. *Appl. Catal. B: Environ.* **2021**, *289*, 120039.
[52] Xu, F. Y.; Meng, K.; Cheng, B.; Wang, S. Y.; Xu, J. S.; Yu, J. G. Unique S-scheme heterojunctions in self-assembled TiO_2/$CsPbBr_3$ hybrids for CO_2 photoreduction. *Nat. Commun.* **2020**, *11*, 4613.
[53] Wang, L. B.; Fei, X. G.; Zhang, L. Y.; Yu, J. G.; Cheng, B.; Ma, Y. H. Solar fuel generation over nature-inspired recyclable TiO_2/g-C_3N_4 S-scheme hierarchical thin-film photocatalyst. *J. Mater. Sci. Technol.* **2022**, *112*, 1–10.
[54] Hu, J. D.; Yang, T. Y.; Yang, X. G.; Qu, J. F.; Cai, Y. H.; Li, C. M. Highly selective and efficient solar-light-driven CO_2 conversion with an ambient-stable 2D/2D Co_2P@BP/g-C_3N_4 heterojunction. *Small* **2022**, *18*, 2105376.
[55] Wang, L.; Wang, L.; Xu, Y. K.; Sun, G. X.; Nie, W. C.; Liu, L. H.; Kong, D. B.; Pan, Y.; Zhang, Y. H.; Wang, H. et al. Schottky junction and D-A_1-A_2 system dual regulation of covalent triazine frameworks for highly efficient CO_2 photoreduction. *Adv. Mater.* **2024**, *36*, 2309376.
[56] Wisser, F. M.; Duguet, M.; Perrinet, Q.; Ghosh, A. C.; Alves-Favaro, M.; Mohr, Y.; Lorentz, C.; Quadrelli, E. A.; Palkovits, R.; Farrusseng, D. et al. Molecular porous photosystems tailored for

long-term photocatalytic CO_2 reduction. *Angew. Chem., Int. Ed.* **2020**, *59*, 5116–5122.

[57] Huang, G. C.; Lin, G. Y.; Niu, Q.; Bi, J. H.; Wu, L. Covalent triazine-based frameworks confining cobalt single atoms for photocatalytic CO_2 reduction and hydrogen production. *J. Mater. Sci. Technol.* **2022**, *116*, 41–49.

[58] Huang, G. C.; Niu, Q.; He, Y. X.; Tian, J. J.; Gao, M. B.; Li, C. Y.; An, N.; Bi, J. H.; Zhang, J. W. Spatial confinement of copper single atoms into covalent triazine-based frameworks for highly efficient and selective photocatalytic CO_2 reduction. *Nano Res.* **2022**, *15*, 8001–8009.

[59] Hu, X. L.; Zheng, L. R.; Wang, S. Y.; Wang, X. Y.; Tan. B. Integrating single Co sites into crystalline covalent triazine frameworks for photoreduction of CO_2. *Chem. Commun.* **2022**, *58*, 8121–8124.

[60] Yi, J. D.; Li, Q. X.; Chi, S. Y.; Huang, Y. B.; Cao, R. Boron-doped covalent triazine framework for efficient CO_2 electroreduction. *Chem. Res. Chin. Univ.* **2022**, *38*, 141–146.

[61] Suo, X.; Zhang, F. T.; Yang, Z. Z.; Chen, H.; Wang, T.; Wang, Z. Y.; Kobayashi, T.; Do-Thanh, C. L.; Maltsev, D.; Liu, Z. M. et al. Highly perfluorinated covalent triazine frameworks derived from a low-temperature ionothermal approach towards enhanced CO_2 electroreduction. *Angew. Chem., Int. Ed.* **2021**, *60*, 25688–25694.

[62] Wang, C. X.; Zhang, H. L.; Luo, W. J.; Sun, T.; Xu, Y. X. Ultrathin crystalline covalent-triazine-framework nanosheets with electron donor groups for synergistically enhanced photocatalytic water splitting. *Angew. Chem., Int. Ed.* **2021**, *60*, 25381–25390.

[63] Gao, P. P.; Wu, C. B.; Wang, S. Y.; Zheng, G. F.; Han, Q. Efficient photosynthesis of hydrogen peroxide by triazole-modified covalent triazine framework nanosheets. *J. Colloid Interface Sci.* **2023**, *650*, 40–46.

[64] Huang, G. C.; Niu, Q.; Zhang, J. W.; Huang, H. M.; Chen, Q. S.; Bi, J. H.; Wu, L. Platinum single-atoms anchored covalent triazine framework for efficient photoreduction of CO_2 to CH_4. *Chem. Eng. J.* **2022**, *427*, 131018.

[65] Tao, Y.; Yang, D. H.; Kong, H. Y.; Wang, T. X.; Li, Z. H.; Ding, X. S.; Han, B. H. Covalent triazine polymer derived porous carbon with high porosity and nitrogen content for bifunctional oxygen catalysis in zinc-air battery. *Appl. Catal. B: Environ.* **2023**, *339*, 123088.

[66] Li, N. N.; Tang, R. Z.; Su, Y. Z.; Lu, C. B.; Chen, Z. M.; Sun, J.; Lv, Y. Q.; Han, S.; Yang, C. Q.; Zhuang, X. D. Isometric covalent triazine framework-derived porous carbons as metal-free electrocatalysts for the oxygen reduction reaction. *ChemSusChem* **2023**, *16*, e202201937.

[67] Zheng, Y.; Chen, S.; Zhang, K. A. I.; Zhu, J. X.; Xu, J. S.; Zhang, C.; Liu, T. X. Ultrasound-triggered assembly of covalent triazine framework for synthesizing heteroatom-doped carbon nanoflowers boosting metal-free bifunctional electrocatalysis. *ACS Appl. Mater. Interfaces* **2021**, *13*, 13328–13337.

[68] Allwyn, N.; Ambrose, B.; Kathiresan, M.; Sathish, M. Self-sacrificial templated nanoarchitectonics of nitrogen-doped carbon derived from viologen-based covalent triazine polymer: An oxygen reduction electrocatalyst in zinc-air batteries. *ACS Appl. Energy Mater.* **2023**, *6*, 11408–11419.

[69] Pan, Y.; Xin, Y. P.; Li, Y. H.; Xu, Z.; Tang, C.; Liu, X.; Yin, Y. C.; Zhang, J. C.; Xu, F. G.; Li, C. et al. Nitrogen-doped carbon cubosomes as an efficient electrocatalyst with high accessibility of internal active sites. *ACS Nano* **2023**, *17*, 23850–23860.

[70] Song, K. S.; Talapaneni, S. N.; Ashirov, T.; Coskun, A. Molten salt templated synthesis of covalent isocyanurate frameworks with tunable morphology and high CO_2 uptake capacity. *ACS Appl. Mater. Interfaces* **2021**, *13*, 26102–26108.

[71] Sun, L.; Yang, M.; Guo, H.; Zhang, T. T.; Wu, N.; Wang, M. Y.; Yang, F.; Zhang, J. Y.; Yang, W. COOH-MWCNT connected COF and chemical activated CTF as a novel electrochemical sensing platform for simultaneous detection of acetaminophen and p-aminophenol. *Colloids Surf. A Physicochem. Eng. Aspects* **2022**, *647*, 129092.

[72] Sun, L.; Guo, H.; Pan, Z. L.; Liu, B. Q.; Wu, N.; Liu, Y. S.; Lu, Z. Y.; Wei, X. Q.; Yang, W. Design of $NiCo_2O_4$ nanoflowers decorated sulfurbridged covalent triazine frameworks nanocomposites for electrochemical simultaneous detection of acetaminophen and 4-aminophenol. *Microchem. J.* **2022**, *182*, 107879.

[73] Zhu, X. J.; Dai, J. L.; Li, L. G.; Wu, Z. X.; Chen, S. W. N. S-codoped hierarchical porous carbon spheres embedded with cobalt nanoparticles as efficient bifunctional oxygen electrocatalysts for rechargeable zinc-air batteries. *Nanoscale* **2019**, *11*, 21302–21310

[74] Li, M. J.; Lv, M. H.; Zheng, Y.; Zhu, M. M.; Feng, Q. C.; Guan, J. Y.; Yu, X. H.; Shen, Y.; Hou, J. H.; Lu, Y. et al. Bimetallic-coordinated covalent triazine framework-derived FeNi alloy nanoparticle-decorated coral-like nanocarbons for oxygen electrocatalysis. *ACS Appl. Mater. Interfaces* **2024**, *16*, 633–642.

[75] Zhu, Y. Z.; Chen, X. F.; Liu, J.; Zhang, J. F.; Xu, D. Y.; Peng, W. C.; Li, Y.; Zhang, G. L.; Zhang, F. B.; Fan, X. B. Rational design of Fe/N/S-doped nanoporous carbon catalysts from covalent triazine frameworks for efficient oxygen reduction. *ChemSusChem* **2018**, *11*, 2402–2409.

[76] Zheng, Y.; Chen, S.; Zhang, K. A. I.; Guan, J. Y.; Yu, X. H.; Peng, W.; Song, H.; Zhu, J. X.; Xu, J. S.; Fan, X. S. et al. Template-free construction of hollow mesoporous carbon spheres from a covalent triazine framework for enhanced oxygen electroreduction. *J. Colloid Interface Sci.* **2022**, *608*, 3168–3177.

[77] Jena, H. S.; Krishnaraj, C.; Satpathy, B. K.; Rawat, K. S.; Leus, K.; Veerapandian, S.; Morent, R.; De Geyter, N.; Van Speybroeck, V.; Pradhan, D. et al. Phosphorus covalent triazine framework-based nanomaterials for electrocatalytic hydrogen evolution reaction. *ACS Appl. Nano Mater.* **2023**, *6*, 22684–22692.

[78] Zhang, J.; Xu, Y. P.; Lan, M. W.; Wang, X. D.; Fu, N.; Yang, Z. L. Heteroatom-doped carbon materials derived from covalent triazine framework@MOFs for the oxygen reduction reaction. *Dalton Trans.* **2022**, *51*, 14482–14490.

[79] Khan, R.; Chakraborty, J.; Rawat, K. S.; Morent, R.; De Geyter, N.; Van Speybroeck, V.; Van Der Voort, P. Super-oxidizing covalent triazine framework electrocatalyst for two-electron water oxidation to H_2O_2. *Angew. Chem., Int. Ed.* **2023**, *62*, e202313836.

[80] Huo, L. P.; Lv, M. H.; Li, M. J.; Ni, X. P.; Guan, J. Y.; Liu, J.; Mei, S. X.; Yang, Y. Q.; Zhu, M. M.; Feng, Q. C. et al. Amorphous MnO_2 lamellae encapsulated covalent triazine polymer-derived multi-heteroatoms-doped carbon for ORR/OER bifunctional electrocatalysis. *Adv. Mater.* **2024**, *36*, 2312868.